

1
2
3
4
5
6
7
8
9
10
11

Supporting Information for
Catchment landforms predict groundwater-dependent wetland sensitivity to
recharge changes

Etienne Marti¹, Sarah Leray^{1,2}, Clément Roques^{3,*}

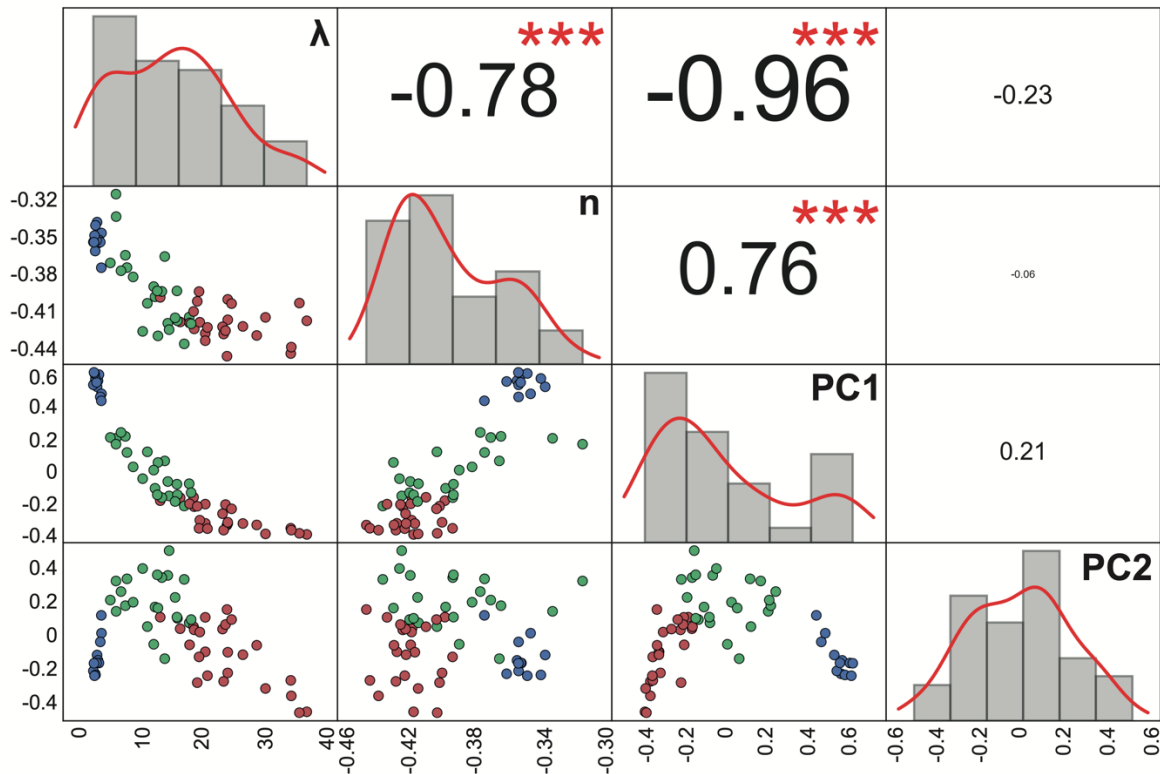
¹ Departamento de Ingeniería Hidráulica y Ambiental, Pontificia Universidad Católica de Chile, Santiago, Chile

² Centro de Cambio Global UC, Santiago, Chile

³ CHYN, University of Neuchâtel, Neuchâtel, Switzerland

* Corresponding author

12 S1: Correlation matrix between topographical parameters and seepage
 13 distribution parameters



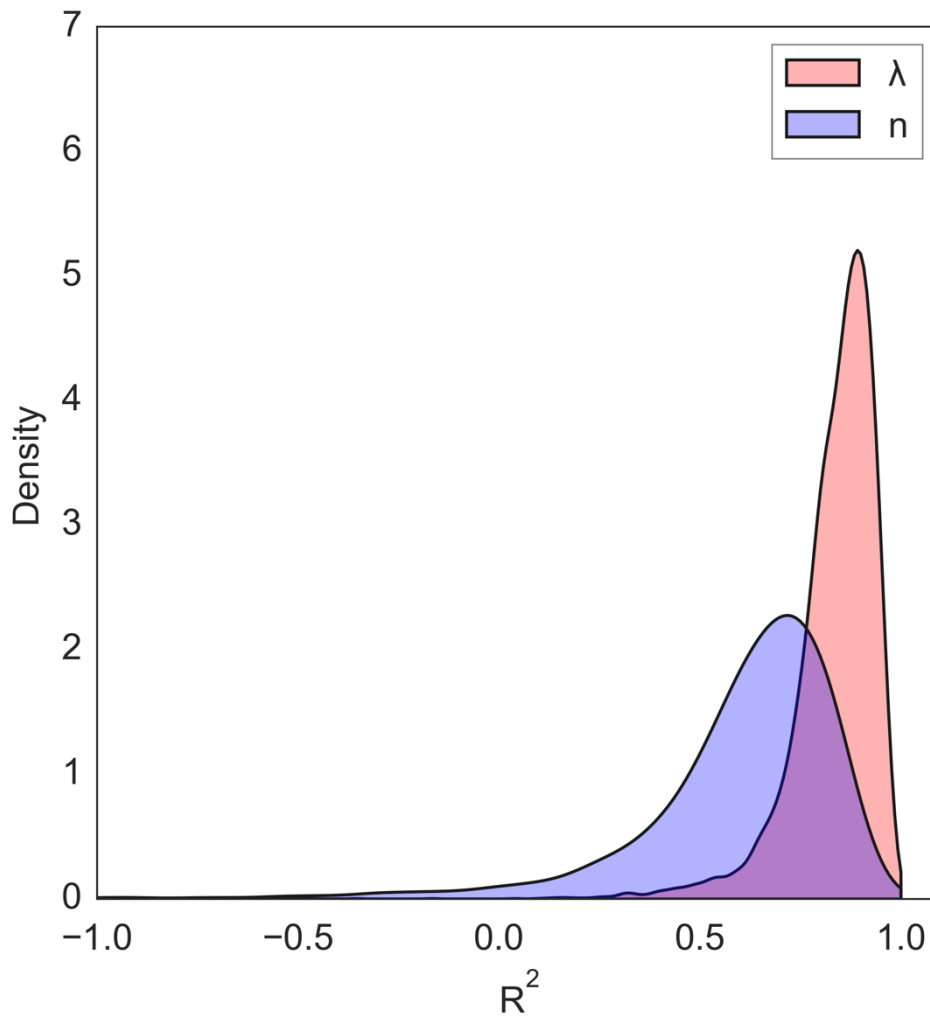
14

15 *Figure S1 Correlation matrix between topographical parameters (PC1 and PC2) and seepage*
 16 *distribution parameters (λ and n) obtained from the curve fit. The diagonal part represents the distribution of each parameter associated with its name. The*
 17 *upper part indicates the correlation coefficient (r) between two variables, with stars indicating the strength of the correlation*
 18 *on a scale from 0 to 3 (for 3 stars p-value<0.001). The lower part represents the scatter plot between the two corresponding*
 19 *variables using the clusters color scheme. The X-axis is associated with both the scatter plots and the histogram distribution,*
 20 *while the Y-Axis is only associated with the scatter plots.*

21

22 S2: Kernel Density Estimate

23 For the prediction of lambda, we obtained an R2 mean value of 0.835 within a 95% confidence
24 interval defined as [0.832-0.838] and a median value of 0.858. As for n, we obtained an R2
25 mean value of 0.584 within a 95% confidence interval defined as [0.575-0.593] and a median
26 value of 0.658.

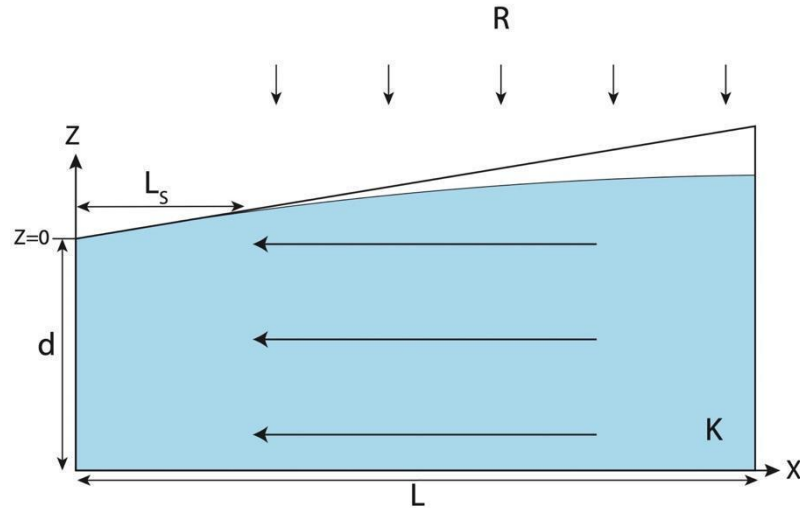


27

28 *Figure S2 Kernel Density Estimate (KDE) plot depicting the coefficient of determination (R^2) for parameter estimations of*
29 *λ and n using a Random Forest algorithm. Each R^2 value corresponds to one of 5000 resampling (with replacements) iterations*
30 *involving 10 basins, serving as test data within a 60-basin dataset, while 50 basins were utilized for training. The sampling*
31 *procedure was conducted to assess the estimation's robustness in the presence of random variations.*

32

33 S3: Framework for 2D analytical solutions and sensitivity analysis of solution
 34 parameters



35

36 *Figure S3 Illustration of the 2D hillslope model employed to define the analytical solution, based on Bresciani et al. (2014).*

37

38 Bresciani et al. (2014) devised an analytical approach based on the Dupuit-Forchheimer
 39 assumption to estimate seepage length in hillslopes. This particular hillslope scenario is
 40 depicted in Figure S3, where d [L] represents the depth to the impervious base beneath the
 41 streambed, L [L] denotes the hillslope length, L_s [L] the seepage length, K [LT^{-1}] the hydraulic
 42 conductivity, R [LT^{-1}] the available recharge rate, and s [-] the topographic slope.

43 In this 2D hillslope framework, the model top (Z_T) is represented as a constant slope
 44 topography:

45
$$Z_T(x) = sx$$

 46 with s [-] the topographic slope.

47

48 For this case the ratio between seepage length and hillslope length is defined, by mass
 49 balance, as:

50
$$\frac{L_s}{L} = \frac{1 - \frac{sKd}{RL}}{1 + \frac{s^2K}{R}}$$

51

52 To delve deeper into the geomorphological impact and introduce complexity beyond the
 53 constant slope framework, Bresciani et al. (2014) introduced variable slope topography,
 54 including the concave case:

$$55 \quad Z_{Tconcave}(x) = sx + \frac{1}{2}bx^2$$

56 Or convex case:

$$57 \quad Z_{Tconvex}(x) = sx - \frac{1}{2}bx^2$$

58 With b [-] the curvature degree.

59 Here, we expand this work with the Dupuit solution seepage length estimation from the three
 60 different cases. For comparison purpose, we introduce a constraint on topography borders
 61 as:

$$62 \quad Z_T(x = 0) = Z_{Tconcave}(x = 0) = Z_{Tconvex}(x = 0)$$

63 And:

$$64 \quad Z_T(x = L) = Z_{Tconcave}(x = L) = Z_{Tconvex}(x = L)$$

65

66 To take this constraint into account, we need to accommodate the expression of the concave
 67 and convex topography:

$$68 \quad \Rightarrow Z_{Tconcave}(x) = \frac{2s - bL}{2}x + \frac{1}{2}bx^2$$

$$69 \quad \Rightarrow Z_{Tconvex}(x) = \frac{2s + bL}{2}x - \frac{1}{2}bx^2$$

70

71 Resolving the same mass balance as for the linear case, for the concave and convex cases, the
 72 seepage length (L_S/L) is determined as the real roots of the following 3rd degree polynomials:

73 For concave case:

$$74 \quad \frac{1}{2}(bL)^2 \left(\frac{L_S}{L}\right)^3 + \frac{3bL(2s - bL)}{4} \left(\frac{L_S}{L}\right)^2 + \left(\frac{R}{K} + \frac{(2s - bL)^2}{4} + \frac{d}{L}bL\right) \left(\frac{L_S}{L}\right) + \frac{(2s - bL)d}{2} \frac{d}{L} - \frac{R}{K} = 0$$

75

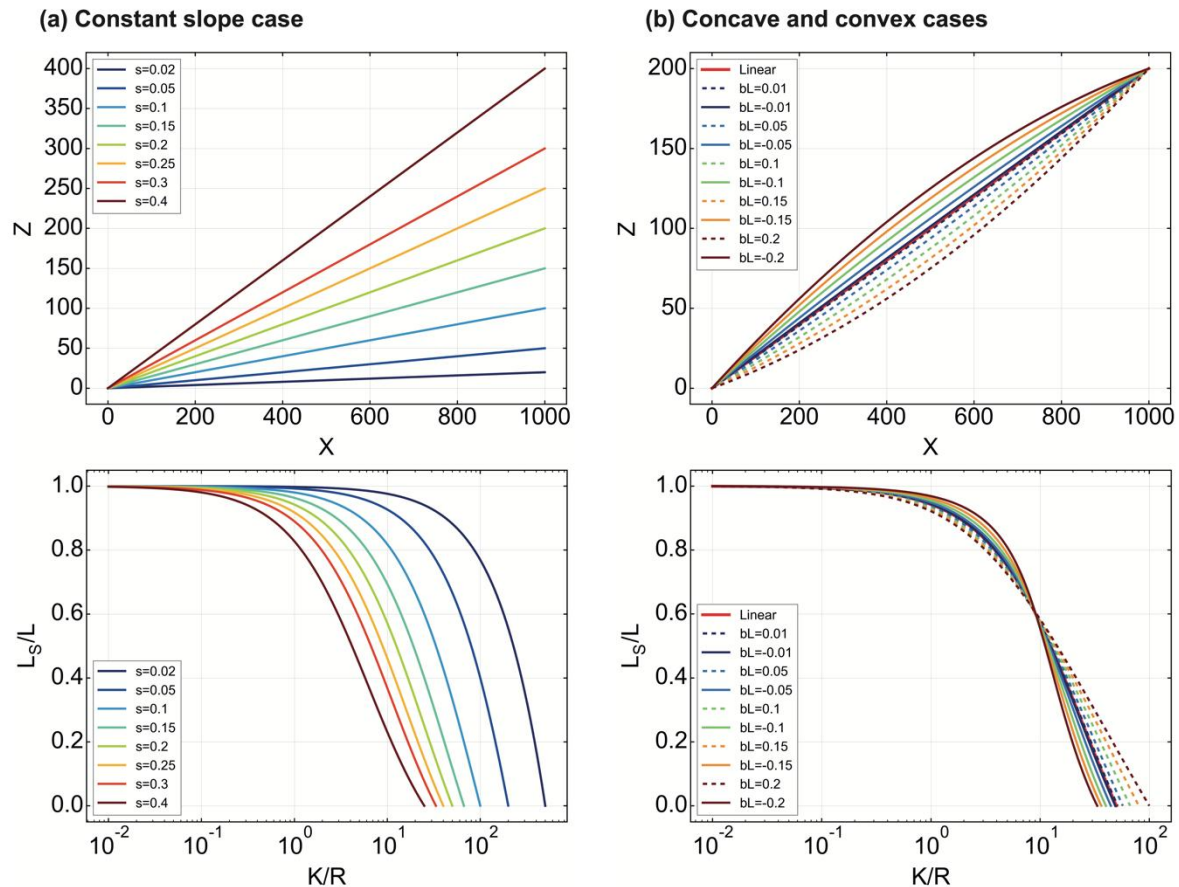
76 For convex case:

$$\frac{1}{2}(bL)^2 \left(\frac{L_S}{L}\right)^3 - \frac{3bL(2s + bL)}{4} \left(\frac{L_S}{L}\right)^2 + \left(\frac{R}{K} + \frac{(2s + bL)^2}{4} - \frac{d}{L}bL\right) \left(\frac{L_S}{L}\right) + \frac{(2s + bL)d}{2} \frac{d}{L} - \frac{R}{K} = 0$$

78

79 In this study, our primary focus was on the L_S/L ratio in comparison to the K/R ratio. To
 80 comprehensively investigate the analytical solution, we conducted a sensitivity analysis on
 81 the slope parameter, which serves as the most significant indicator of topography in this
 82 specific case. For this analysis, the hillslope length (L) was set to 1000m, and the depth to
 83 impervious base (d) was maintained at $d=100m$ to respect the ratio $d/L=0.1$ and to consider
 84 the Dupuit Forchheimer condition ($d/L < 0.2$) (Bresciani et al., 2014; Haitjema & Mitchell-
 85 Bruker, 2005). We considered a range of slope values, spanning [0.02, 0.05, 0.1, 0.15, 0.2,
 86 0.25, 0.3, 0.4].

87 To further explore the effects of these cases, we conducted a sensitivity study on the
 88 curvature degree. For this analysis, we maintained a fixed slope ($s=0.2$), and the curvature
 89 degree multiplied by the hillslope length (bL) was varied in the range [0.01, 0.05, 0.1, 0.15,
 90 0.2] for the concave case and in the opposite range [-0.01, -0.05, -0.1, -0.15, -0.2] for the
 91 convex case.



92

93 *Figure S4 (a) Left upper panel: Topography of the hillslope Z_T , with each color corresponding to a different slope value. Left*
 94 *lower panel: Seepage length ratio L_S/L plotted against the ratio R/K for each hillslope case presented on the left upper panel*
 95 *using the same color palette. (b) Right upper panel: Topography of the hillslope Z_T , with each color corresponding to a different*
 96 *curvature degree value. Dashed lines represent concave cases, and solid lines represent convex cases. The linear case is*
 97 *represented by a solid red line. Right lower panel: Seepage length ratio L_S/L plotted against the ratio R/K for each hillslope*
 98 *case presented on the right upper panel, using the same color palette and line patterns.*

99

100 Figure S4 presents the results of the sensitivity study with the slope (s) for the left panel and
 101 curvature degree (bL) on the right panel. The lower panel of Figure S4 presents the ratio L_S/L
 102 for the various topography described on the upper panel plotted against the ratio K/R .
 103 Regarding the varying slope (s) on the left panel of Figure S4, the results show that slope
 104 incrementation exhibits a linear effect, with gentler slopes remaining fully saturated for a
 105 higher number of K/R and reaching $L_S/L = 0$ for the highest value of K/R . In contrast, steeper
 106 slopes desaturate at lower K/R and intercept $L_S/L = 0$ for the smallest value of K/R . The right
 107 panel of Figure S4 displays the results for the concave and convex cases. In terms of seepage

108 length, we observed distinct behaviors between concave and convex topography, with more
109 pronounced effects as the degree of curvature increased. In the convex hillslope case,
110 remains fully saturated for a higher K/R , but the desaturation rate become quicker, leading
111 to full desaturation ($L_s/L=0$) before the linear case. Conversely, desaturation occurred earlier
112 in the concave hillslope cases (lower K/R), but with a slower rate, indicating that they reached
113 total desaturation ($L_s/L=0$) beyond the linear case.

114 Overall, we noticed that the curvature degree has a secondary influence on the seepage
115 length compared to the slope value (Figure S4 left versus right panel). Nevertheless, there is
116 a noteworthy effect of the curvature degree on the desaturation rate of the hillslope.

117